

Making Images Undiscoverable from Co-Saliency Detection

Ruijun Gao^{1*}, Qing Guo^{2*†}, Felix Juefei-Xu³, Hongkai Yu⁴, Xuhong Ren⁵,
Wei Feng^{1†}, Song Wang^{1,6}

¹ College of Intelligence and Computing, Tianjin University, China

² Nanyang Technological University, Singapore

³ Alibaba Group, USA

⁴ Cleveland State University, USA

⁵ Tianjin University of Technology, China

⁶ University of South Carolina, USA

Abstract

In recent years, co-saliency object detection (CoSOD) has achieved significant progress and played a key role in the retrieval-related tasks, *e.g.*, image retrieval and video foreground detection. Nevertheless, it also inevitably posts a totally new safety and security problem, *i.e.*, how to prevent high-profile and personal-sensitive contents from being extracted by the powerful CoSOD methods. In this paper, we address this problem from the perspective of adversarial attack and identify a novel task, *i.e.*, *adversarial co-saliency attack*: given an image selected from an image group containing some common and salient objects, how to generate an adversarial version that can mislead CoSOD methods to predict incorrect co-salient regions. Note that, compared with general adversarial attacks for classification, this new task introduces *two extra challenges* for existing whitebox adversarial noise attacks: (1) low success rate due to the diverse appearance of images in the image group; (2) low transferability across CoSOD methods due to the considerable difference between CoSOD pipelines. To address these challenges, we propose the very first blackbox *joint adversarial exposure & noise attack (Jadena)* where we jointly and locally tune the exposure and additive perturbations of the image according to a newly designed *high-feature-level contrast-sensitive loss* function. Our method, without any information of the state-of-the-art CoSOD methods, leads to significant performance degradation on various co-saliency detection datasets and make the co-salient objects undetectable, which can be strongly practical in nowadays where large-scale personal photos are shared on the internet and should be properly and securely preserved.

1 Introduction

Co-saliency is commonly referred to as the common and salient (usually in foreground) visual stimulus residing in a given image group. Co-saliency object detection (CoSOD) therefore aims at detecting and highlighting the common and salient foreground region (object) in the said image group (Zhang et al. 2018). Different from the traditional single-image saliency detection problem, the key to solving the co-saliency problem is to discover the correspondence (based

*Ruijun Gao and Qing Guo are co-first authors and contribute equally to this work.

†Wei Feng and Qing Guo are the corresponding authors: wfeng@ieee.org, tsingqguo@gmail.com.

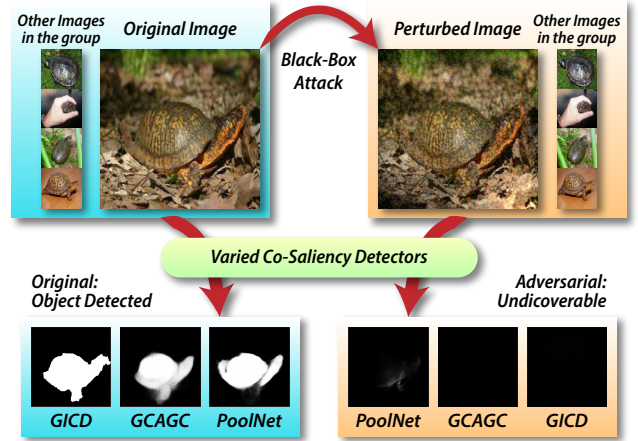


Figure 1: An overall of the novel problem and our solution. We expect the perturbed image to be undiscoverable in an even dynamically growing group of images across multiple CoSOD methods, which is much more challenging and practical in real-world scenarios. Note that, our attack is black-box and can be performed without references provided in the group.

on various cues) for the common and similar salient region among multiple images in an image group. With unknown semantic categories of the co-salient objects, the co-saliency task is a rather challenging one, and a good co-saliency detection algorithm should consider both the intra-image saliency cues and the inter-image common saliency cues (Fu, Cao, and Tu 2013).

At the moment, the co-saliency detection is still an emerging research direction, with many newly proposed methods to solve this challenging problem. We will detail many of the CoSOD algorithms ranging from low-level features to high-level semantic features, as well as deep learning based ones in Section 2. Co-saliency detection plays a key role in many practical applications surrounding computer vision and multimedia such as object co-segmentation (Zhu et al. 2016), foreground discovery in video sequences (Chang et al. 2015), weakly supervised localization (Zhang et al. 2016), image retrieval (Fu, Cao, and Tu 2013), multi-camera

surveillance (Luo et al. 2015), 3D object reconstruction from 2D images (Kar et al. 2015), etc.

However, the many existing powerful CoSOD methods inevitably pose a fairly new safety and security problem, *i.e.*, high-profile and personal-sensitive contents may be subject to extraction and discovery by the CoSOD methods. In order to prevent content-sensitive images from being discovered by co-saliency detection, in this work, we address the problem from the perspective of adversarial attack and identify a novel task, *i.e.*, adversarial co-saliency attack that aims at tackling the following scenario: given an image selected from an image group containing some common and salient objects, how to generate an adversarial version of the image that can mislead CoSOD methods to predict incorrect co-salient regions, thus evading the co-saliency detection and making the images undiscoverable by the co-saliency detection algorithms.

It is worth noting that compared with general adversarial attacks for classification, this new task introduces *two extra challenges* for existing whitebox adversarial noise attacks: (1) low success rate due to the diverse appearance of images in the image group; (2) low transferability across CoSOD methods due to the considerable difference between CoSOD pipelines. To overcome these challenges, we propose the very first blackbox **joint adversarial exposure & noise attack (Jadena)** where we jointly and locally tune the exposure and additive perturbations of the image according to a newly designed *high-feature-level contrast-sensitive loss* function. Our method, without needing any information of the state-of-the-art CoSOD methods, leads to significant performance degradation on various co-saliency detection datasets and make the co-salient objects undetectable, as shown in Fig. 1, which can be strongly practical in nowadays where large-scale personal multimedia contents are shared on the public domain Internet and should be properly and securely preserved and protected from malicious extraction.

2 Related Work

In this section, we will introduce the related work of co-saliency detection, adversarial attack, and adversarial attack for saliency detection.

2.1 Co-saliency Detection

As an important branch of the saliency detection researches (Achanta et al. 2009; Cheng et al. 2015; Li and Yu 2015, 2016; Wang et al. 2016; Qin et al. 2019; Song et al. 2020), the mainstream co-saliency detection problem aims to detect the common/similar salient objects in a group of multiple images (Yu et al. 2018; Jiang et al. 2019; Li et al. 2019; Zhang et al. 2020c,a; Zha et al. 2020). Co-saliency detection not only considers the inter-image saliency cue but also the inter-image common saliency cue (Fu, Cao, and Tu 2013; Ge et al. 2016). Discovering the correspondence for the common/similar objects among multiple images is the key to the co-saliency detection, which is solved by several optimization based methods (Cao et al. 2014; Li et al. 2014), machine learning based methods (Cheng et al. 2014; Zhang et al. 2015), and deep neural networks based methods (Zhang

et al. 2020c,a; Zha et al. 2020). In addition, other modality data like the depth image could be fused to improve the RGB color image based co-saliency detection (Cong et al. 2018). Co-saliency detection has a lot of practical applications in computer vision and multimedia areas, such as the co-segmentation (Jerriothula, Cai, and Yuan 2018) and co-localization (Tang et al. 2014), that segments and localizes the similar objects in a group of multiple images.

2.2 Adversarial Attack

As the booming development of deep neural networks, the model safety attracts more and more attentions, therefore many research works have been proposed for the adversarial attack applied to the deep neural networks. Among these works, several classical methods already show promising results, such as the fast gradient signed method (FGSM) (Goodfellow, Shlens, and Szegedy 2014), basic iterative method (BIM) (Kurakin, Goodfellow, and Bengio 2016), C&W method (Carlini and Wagner 2017), momentum iterative fast gradient sign method (MI-FGSM) (Dong et al. 2018), and so on. On one hand, most of current adversarial attacks make efforts to learn an additive noise as a white-box setting when the model parameters are given. For example, the learnable noises will be added to the clean image as a perturbation so as to drop the task performance. On the other hand, some other researches try to simulate the perturbation in the real-world applications with imperceptible human visual sense, such as the motion blur based attack (Guo et al. 2020b) and the watermark based attack (Jia et al. 2020). The proposed method is different with these methods mentioned above because it is a kind of non-additive-noise attack for the black-box setting.

2.3 Adversarial Attack for Saliency Detection

Currently, there are not many research works of adversarial attack and defense for the salient object detection. (Tran et al. 2020) shows that adding adversarial attacks, *e.g.*, using FGSM (Goodfellow, Shlens, and Szegedy 2014), will result in a significant performance drop in saliency detection, so (Tran et al. 2020) proposed a method to clean data affected by an adversarial attack. Different with image-space attacks, (Che et al. 2019) proposed a sparser feature-space adversarial perturbation against the deep saliency models that just requires a part of model information. To the best of our knowledge, this paper is the first work of the adversarial attack for the co-saliency detection.

3 Methodology

3.1 Problem Formulation

Co-saliency object detection (CoSOD). Given a dynamic image group $\mathcal{I} = \{\mathbf{I}_i\}$ containing $|\mathcal{I}|$ images that have common and salient objects. The ‘dynamic’ means the image group can be dynamically changed or extended since the personal images are updated everyday in the real-world applications. A CoSOD method denoted as $D(\cdot)$ takes the image group as input and outputs the common and salient regions in all images

$$\mathcal{S} = \{\mathbf{S}_i\}_{i=1}^{|\mathcal{I}|} = D(\mathcal{I}), \quad (1)$$

where $\mathbf{S}_i = \mathbf{D}(\mathcal{I})[i]$ is a binary map of the i -th image to represent its common and salient regions with ‘1’ and others with ‘0’. Till now, there are numerous CoSOD methods that have different pipelines and can realize effective co-saliency detection.

Task definition. In this paper, we focus on a totally new problem: given an image \mathbf{I}_k from the dynamic image group \mathcal{I} with $k \in [1, \dots, |\mathcal{I}|]$, how to make it undiscoverable from co-saliency object detection (CoSOD) methods. To solve this problem, we formulate it as the adversarial attack: transferring the image \mathbf{I}_k with adversarial perturbations to fool a CoSOD method $\mathbf{D}(\cdot)$ to predict an incorrect salient map, *i.e.*, \mathbf{S}_k , for \mathbf{I}_k . Specifically, we can add perturbations to the original image \mathbf{I}_k by $\mathbf{I}_k^a = P_\theta(\mathbf{I}_k)$ where \mathbf{I}_k^a is the adversarial example aiming to fool the CoSOD method and $P_\theta(\mathbf{I}_k)$ is a kind of image transformation (*e.g.*, $P_\theta(\mathbf{I}_k) = \mathbf{I}_k + \theta$ for the popular additive-perturbation-based attack). The key for the adversarial attack is how to calculate the parameter θ .

3.2 Adversarial Noise Attack and Challenges

We first consider a straightforward way to achieve the task with the popular additive-perturbation-based attack. To be specific, we define

$$\mathbf{I}_k^a = P_\theta(\mathbf{I}_k) = \mathbf{I}_k + \theta, \quad (2)$$

where θ is the pixel-wise perturbation having the same size with \mathbf{I}_k . Then, we can define the following objective function for calculating θ

$$\arg \max_{\theta} J(\mathbf{D}(\{\mathbf{I}_k + \theta, \mathbf{I}_i | i \neq k\})[k], \mathbf{S}_k),$$

subject to $\|\theta\|_p \leq \epsilon, \quad (3)$

where \mathbf{S}_k is the CoSOD result of \mathbf{I}_k based on the original image group and $J(\cdot)$ is a loss function measuring the distance between the predictive results and \mathbf{S}_k . The constraint function, *i.e.*, $\|\theta\|_p \leq \epsilon$, is used to control the distortion degree determined by θ .

We can optimize above function with the optimizations for additive-perturbation-based attacks, *i.e.*, one-step signed gradient-based, iterative-based, and momentum-based optimization methods. However, we find such general adversarial noise attack cannot accomplish the new task very well since it posts two *challenges*: ❶ it is hard for the white-box adversarial noise attack to reach high attack success rate since the dynamic image group \mathcal{I} make the optimized θ ineffective when new images are added. ❷ since the diverse pipelines of CoSOD the optimized θ has low transferability, that is, the optimized θ based on one CoSOD method fails to fool another one.

3.3 Joint Adversarial Exposure & Noise Attack

In this section, we introduce a new black-box attack method that can address the two challenges that block the white-box adversarial noise attack. In general, the saliency of an object is related to the contrast to other regions of the input image while the contrast is usually affected by exposure that is a common phenomenon during image capture. To realize effective co-saliency attack, in contrast to only considering the noise in Sec. 3.2, we propose to jointly consider exposure and noise factors during attack.

Formulation. We add the joint exposure&noise based perturbations to the image \mathbf{I}_k by

$$\mathbf{I}_k^a = P_\theta(\mathbf{I}_k) = \theta_e \mathbf{I}_k + \theta_n, \quad (4)$$

where $\theta = [\theta_e, \theta_n]$ with θ_e and θ_n denote the pixel-wise exposure and noise matrices, respectively. Note that, the above exposure model has been widely used in various image enhancement based methods (Fu et al. 2016; Zhang et al. 2020b). However, to realize effective co-saliency attack is still challenging: ❶ exposure phenomenon is smooth across the whole image domain and cannot be pixel-wise tuned like the noise otherwise we would get speckle-like appearance. ❷ it is still unknown how to optimize these parameters to achieve black-box attack across different CoSODs.

For the first challenge, we construct an objective function to encourage the naturalness of the exposure. For the second one, instead of optimizing θ based on a CoSOD method, we explore a completely black-box way where we define the objective functions on the high-level features extracted from a pretrained classification model denoted as $\phi(\cdot)$.

Objective function for naturalness of the adversarial exposure. We emphasize that exposure in the real world is usually smooth (*i.e.*, neighboring pixels should have very similar exposure) across the whole image. In contrast, the adversarial attack requires the exposure to can be locally different for high attack success rate. Besides, we want the exposure should modify the original input as less as possible. To meet these requirements, we propose to represent the exposure with the locally-variant multivariate polynomial model in the logarithm domain and have

$$\log(\theta_{e,p}) = \sum_{d=0}^D \sum_{l=0}^{D-d} a_{d,l} (x_p + u_p)^d (y_p + v_p)^l, \quad (5)$$

where x_p & y_p are the coordinates of the p -th pixel. u_p & v_p denotes the variation offsets of the p -th pixel. $\{a_{d,l}\}$ denotes the parameters of polynomial model and is concatenated as \mathbf{a} with D being the degree. Note that, the polynomial model with fewer parameters $\{a_{d,l}\}$ leads to smoother exposure. With Eq. 5, we can represent the exposure as the function of \mathbf{a} and the offset map $\mathbf{U} = \{(u_p, v_p)\}$, *i.e.*, $\theta_e(\mathbf{a}, \mathbf{U})$. More specific, to maintain the smoothness of exposure and let it have the capability of adversarial attack, we define the following objective function

$$J_{\text{smooth}}(\mathbf{a}, \mathbf{U}) = -\lambda_b \|\log(\theta_e(\mathbf{a}, \mathbf{U}))\|_2^2 - \lambda_s \|\nabla \mathbf{U}\|_2^2, \quad (6)$$

where the first term encourages to not perturb the original image \mathbf{I}_k and the second term is a total variation regularization and encourages smooth variation of the exposure.

Objective function against single saliency. We argue that the image \mathbf{I}_k should be perturbed by the exposure and noise to let its high-level features tend to be consistent across all image regions. As a result, the salient objects would be not invisible at high level. To this end, we define the objective function against single saliency

$$J_{\text{cons}}(\mathbf{a}, \mathbf{U}, \theta_n) = -\text{avg}(\{\text{std}(\phi_i(P_\theta(\mathbf{I}_k))) | i \in \mathcal{L}\}) \quad (7)$$

where $\phi_i(\cdot)$ is the i -th layer feature of the CNN $\phi(\cdot)$ and \mathcal{L} denotes the index set of employed layers. The function $\text{std}(\cdot)$ calculates the standard variation of each feature channel and outputs the average of standard variations across all channels. The function $\text{avg}(\cdot)$ computes the average of all $\text{std}(\phi_i(P_\theta(\mathbf{I}_k)))$ across all required layers.

Objective function against co-saliency. Eq. 7 is set to make the object less salient in a single image and may be less effective for co-saliency detection since the non-salient object could be salient again in an image group. We then extend Eq. 7 to the feature level of an image group, *i.e.*, \mathcal{R} with $P_\theta(\mathbf{I}_k) \in \mathcal{R}$, and have

$$J_{\text{co-cons}}(\mathbf{a}, \mathbf{U}, \theta_n) = -\text{avg}(\{\text{std}(\Phi_i(\mathcal{R})) | i \in \mathcal{L}\}), \quad (8)$$

with $\Phi_i(\mathcal{R}) = \text{spl}(\{\phi_i(\mathbf{I}_j) | \mathbf{I}_j \in \mathcal{R}\})$,

where we splice i th-layer features of all images in the \mathcal{R} with the function $\text{spl}(\cdot)$ in a channel-wise way. For example, if the function $\phi_i(\mathbf{I}_j)$ outputs a tensor with size $11 \times 11 \times 256$ for four \mathbf{I}_j in \mathcal{R} , we can get $\Phi_i(\mathcal{R})$ with its size being $44 \times 11 \times 256$. Intuitively, compared with Eq. 7, Eq. 8 is to make the salient regions in \mathbf{I}_k become less salient among the image group \mathcal{R} . Here, we consider two ways for constructing \mathcal{R} . One uses the transformation of \mathbf{I}_k , *e.g.*, rotation and up-down flip; Another employed some other images. We will show that both could realize effective co-saliency attack.

Optimization. With above objective functions, we can calculate the adversarial exposure (*i.e.*, $\theta_e(\mathbf{a}, \mathbf{U})$) and noise (*i.e.*, θ_n) by optimizing

$$\arg \max_{\mathbf{a}, \mathbf{U}, \theta_n} J_{\text{co-cons/cons}}(\mathbf{a}, \mathbf{U}, \theta_n) + J_{\text{smooth}}(\mathbf{a}, \mathbf{U}),$$

subject to $\|\theta_n\|_p \leq \epsilon$. (9)

Compared with the objective function used by adversarial noise attack, *i.e.*, Eq. 3, the new objective function has following advantages: ① our objective function does not rely on CoSOD methods or the networks they used. This means that our method is a totally black-box attack and could be very useful in the practical applications. ② our method is totally unsupervised since it does not use the predicted saliency map *i.e.*, \mathbf{S}_k in Eq. 3, which also make it more useful in the real world. ③ we use the both exposure and noise for more effective attack. We simply use the sign gradient descent algorithm to optimize Eq. 9.

Algorithm. As shown in Fig. 2, our method takes a clean image as input \mathbf{I}_k . In addition to fetching references from an image group, we design another approach, in which \mathbf{I}_k is augmented by flipping, mirroring, left rotation and right rotation to generate four reference images. We collect the original image and references together to consist \mathcal{R} . Then, we initialize coefficients \mathbf{a} of exposure polynomial model, offset map \mathbf{U} and pixel-wise noise θ_n , all with zero values. We will follow Eq. 4 and Eq. 5 to perturb the clean image. Note that, only the original image \mathbf{I}_k is perturbed, other than the reference images. In the situation of initialization, the perturbing is an identity operation. We employ a sign gradient descent algorithm to optimize Eq. 9, and MI-FGSM is adopted in this paper. Finally, the optimized \mathbf{a} , \mathbf{U} and θ_n are

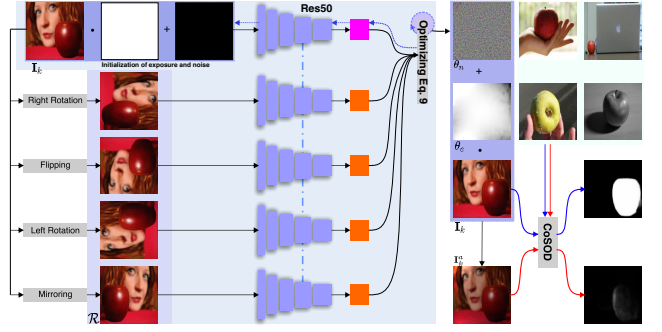


Figure 2: Pipeline of the *joint adversarial exposure and noise attack*. Here shows how the clean image is augmented to generate references by visualization and how the gradient back-propagates along the blue dash lines.

applied to the original clean image, to generate a perturbed image as output, which may fool CoSOD methods.

4 Experiments

In this section, we conduct groups of experiments to evaluate our method and compare it with existing attacks. First, we report the experimental settings in Sec. 4.1. Second, we launch proposed attacks on several CoSOD benchmarks, observe how existing CoSOD methods are affected and perform ablation study to demonstrate the effectiveness of joint perturbation in Sec. 4.2. Last, we compare with existing attack methods on transferability and perceptibility in Sec. 4.3.

4.1 Experimental Setups

Datasets. In this paper, we conduct experiments on Cosal2015 (Zhang et al. 2016), iCoseg (Batra et al. 2010), CoSOD3k (Fan et al. 2020) and CoCA (Zhang et al. 2020c). Cosal2015 and CoSOD3k are large-scale datasets, containing 2015 and 3316 images of 50 and 160 groups. iCoseg contains 643 images of 38 groups, in which objects are in the same scene within a group. CoCA is well-designed for evaluating CoSOD method thanks to having multiple single salient objects in each image, which contains 1295 images of 80 groups.

Models. We involve three CoSOD models and one SOD model for evaluating adversarial attacks. GICD (Zhang et al. 2020c) and GCAGC (Zhang et al. 2020a) are two state-of-the-art CoSOD methods. We employ the GCAGC with an HRNet backbone (Wang et al. 2019). PoolNet (Liu et al. 2019) is a CNN-based SOD method, but here we treat it as a CoSOD method due to its competitive performance on CoSOD datasets. CBCD is a traditional method for both CoSOD and SOD, but we only adopt the co-saliency results in this paper.

Metrics. In our experiments, we employ four metrics to evaluate how adversarial attacks affect detection methods, *i.e.*, Average Precision (AP) (Zhang et al. 2018), F-measure score F_β with $\beta^2 = 0.3$ (Achanta et al. 2009), Mean Absolute Error (MAE) (Zhang et al. 2018) and Success Rate (S). The first three metrics are widely used for CoSOD method

		GICD				GCAGC				CBCD				PoolNet			
		S \uparrow	AP \downarrow	F_β \downarrow	MAE \uparrow	S \uparrow	AP \downarrow	F_β \downarrow	MAE \uparrow	S \uparrow	AP \downarrow	F_β \downarrow	MAE \uparrow	S \uparrow	AP \downarrow	F_β \downarrow	MAE \uparrow
CoSal2015	Original	0.2352	0.8595	0.7800	0.0838	0.1881	0.8960	0.8275	0.0814	0.9504	0.6046	0.1530	0.2287	0.2625	0.8449	0.7626	0.1001
	Jadena _{single}	0.6864	0.7044	0.3831	0.1753	0.4868	0.7682	0.6162	0.1529	0.9663	0.5490	0.1199	0.2354	0.5538	0.6985	0.5152	0.1431
	Jadena _{group}	0.6849	0.7069	0.3838	0.1777	0.5221	0.7453	0.5842	0.1619	0.9826	0.5212	0.0715	0.2392	0.6060	0.6671	0.4650	0.1545
	Jadena _{augment}	0.6893	0.7016	0.3747	0.1749	0.5146	0.7432	0.5960	0.1592	0.9816	0.5137	0.0754	0.2394	0.6010	0.6648	0.4616	0.1513
	Jadena _{augment} w/o noise	0.3226	0.8297	0.7074	0.1037	0.2010	0.8860	0.8182	0.0870	0.9921	0.4853	0.0434	0.2422	0.3677	0.8032	0.6824	0.1145
	Jadena _{augment} w/o exposure	0.5261	0.7536	0.5483	0.1437	0.3821	0.8185	0.7074	0.1243	0.9533	0.6028	0.1473	0.2290	0.4303	0.7680	0.6347	0.1240
iCoseg	Original	0.2970	0.8189	0.7761	0.0851	0.1991	0.8721	0.8036	0.0788	0.7760	0.8005	0.4470	0.1744	0.2286	0.8845	0.7955	0.0709
	Jadena _{single}	0.6952	0.7063	0.4231	0.1666	0.3142	0.8369	0.7257	0.1111	0.8383	0.7422	0.3621	0.1849	0.5381	0.7677	0.5576	0.1346
	Jadena _{group}	0.6874	0.7070	0.4242	0.1663	0.3453	0.8167	0.7046	0.1166	0.9036	0.7073	0.2425	0.1979	0.5848	0.7474	0.4986	0.1450
	Jadena _{augment}	0.7092	0.7017	0.3966	0.1708	0.3733	0.8130	0.6989	0.1178	0.9051	0.7089	0.2324	0.1961	0.5785	0.7351	0.5002	0.1435
	Jadena _{augment} w/o noise	0.3997	0.7905	0.7171	0.1038	0.1975	0.8636	0.8015	0.0821	0.9425	0.6434	0.1361	0.2068	0.3515	0.8456	0.6965	0.0957
	Jadena _{augment} w/o exposure	0.5490	0.7525	0.5593	0.1406	0.2457	0.8626	0.7736	0.0919	0.7916	0.7998	0.4307	0.1750	0.3670	0.8405	0.7051	0.1020
CoSOD3k	Original	0.3555	0.7963	0.6981	0.0927	0.2995	0.8273	0.7672	0.0949	0.9717	0.5184	0.1400	0.2024	0.3667	0.7717	0.6947	0.1164
	Jadena _{single}	0.7630	0.6592	0.3282	0.1613	0.6092	0.6878	0.5481	0.1519	0.9795	0.4692	0.1080	0.2070	0.6622	0.6065	0.4425	0.1513
	Jadena _{group}	0.7672	0.6600	0.3158	0.1638	0.6441	0.6630	0.5125	0.1589	0.9873	0.4411	0.0632	0.2095	0.7156	0.5681	0.3823	0.1579
	Jadena _{augment}	0.7741	0.6544	0.3075	0.1630	0.6360	0.6601	0.5153	0.1586	0.9879	0.4400	0.0741	0.2096	0.7189	0.5614	0.3827	0.1590
	Jadena _{augment} w/o noise	0.4484	0.7657	0.6307	0.1075	0.3139	0.8154	0.7467	0.0993	0.9934	0.4119	0.0341	0.2095	0.4756	0.7192	0.6124	0.1265
	Jadena _{augment} w/o exposure	0.6345	0.6959	0.4627	0.1404	0.5069	0.7361	0.6235	0.1316	0.9744	0.5158	0.1367	0.2030	0.5516	0.6779	0.5530	0.1376
CoCA	Original	0.6680	0.5993	0.4939	0.1187	0.6062	0.5855	0.5970	0.1153	0.9606	0.3543	0.1738	0.1377	0.7259	0.4923	0.4707	0.1681
	Jadena _{single}	0.8046	0.5332	0.3650	0.1265	0.7660	0.4733	0.4893	0.1315	0.9737	0.3228	0.1455	0.1401	0.7954	0.4283	0.3829	0.1320
	Jadena _{group}	0.8340	0.5327	0.3335	0.1226	0.7915	0.4542	0.4584	0.1341	0.9876	0.2998	0.0974	0.1380	0.8355	0.3853	0.3221	0.1271
	Jadena _{augment}	0.8363	0.5284	0.3365	0.1224	0.7876	0.4588	0.4502	0.1347	0.9846	0.2973	0.0995	0.1392	0.8270	0.3909	0.3399	0.1284
	Jadena _{augment} w/o noise	0.6996	0.5852	0.4664	0.1120	0.6100	0.5737	0.5963	0.1179	0.9876	0.2833	0.0643	0.1352	0.7560	0.4571	0.4394	0.1541
	Jadena _{augment} w/o exposure	0.7490	0.5535	0.4310	0.1250	0.7112	0.5244	0.5536	0.1222	0.9691	0.3526	0.1672	0.1385	0.7598	0.4588	0.4428	0.1405

Table 1: Attack performance. “Orginal” means that we predict the co-saliency map of clean images using each CoSOD method. Jadena_{single, augment, group} indicates which variant of Jadena is used, and “w/o noise” or “w/o exposure” means that the attack is performed without additive noise or exposure tuning. We highlight top results of each CoSOD method and each dataset with **red**.

evaluations, and then we may evaluate adversarial attacks by observing how they change from the original performance. The last one, success rate, aims to evaluate the ability of an attack to make images undiscoverable. We treat an attack as a success, when the IoU between the result of a perturbed image and the corresponding ground-truth map is less than 0.5. To calculate Success Rate, we simply divide the total number of results by the number of success result. IoU, *i.e.* Intersection over Union, is widely used in tasks of object detection and visual tracking, and defined as $\text{IoU} = \frac{\text{Area of Overlap}}{\text{Area of Union}}$. Furthermore, for measuring the quality of perturbed images and perceptibility of the applied perturbations, we employ a no-reference image quality assessor, *i.e.*, BRISQUE (Mittal, Moorthy, and Bovik 2011). A smaller BRISQUE score suggests better quality of an image.

4.2 Attack Performance & Ablation Study

We perform our method on several datasets and use four CoSOD methods to predict result maps for the generated adversarial examples. We evaluate three variants of our proposed attack, with different reference choice strategies to build an image group around the attacked image, *i.e.*, no references, references from the same group and augmented references of original images, denoted by Jadena_{single, group, augment}, respectively. The augmentation of original images contains flipping, mirroring, left rotation and right rotation, which is designed for totally black-box attack, even without images of the same group provided. We optimize Eq. 7 for the first variant and Eq. 8 for the other two variants. Moreover, we perform Jadena_{augment} without additive noise perturbation or exposure tuning, and report them as Jadena_{augment} w/o noise and Jadena_{augment} w/o exposure.

For feature extraction required by the adversarial loss computation, we employ a general classification model, ResNet50 (He et al. 2016), and adopt the outputs of stage-

{1, 2, 3}. For the optimization of our proposed adversarial loss, we use MI-FGSM and adopt $\mu = 1.0$ for momentum decay. For other hyperparameters of proposed method, we set the iteration number $N = 20$, $\alpha_n = 1$ w.r.t. pixel values in $[0, 255]$ and maximum noise-perturbation $\epsilon = 16$, which is the same with additive-perturbation-based attack in usual. For the step size of exposure coefficients and the offset map, we use $\alpha_a = 0.1$ and $\alpha_U = 0.01$. For smoothing the exposure tuning, we use $\lambda_b = 0.5$ for the single variant while $\lambda_b = 0.01$ for augment or group variant, $\lambda_s = 0.01$ and polynomial degree $D = 10$, concerning both attack success rate and imperceptibility of perturbations. We report the performance results across CoSOD methods in Tab. 1.

We observe that Jadena_{augment} and Jadena_{group} achieve the best performance on most metrics. Even without sampling images from the same group and only with augmentation of original images, Jadena_{augment} may hold a competitive performance with Jadena_{group} for GCAGC and PoolNet, and outperform Jadena_{group} for GICD. It demonstrates that references provided are not necessary, which may be obtained by augmentation. Jadena_{augment} performs better than “w/o noise” and “w/o exposure” versions except for the CBCD method, which suggests our proposed joint perturbation plays an important role in fooling CoSOD methods. While it is hard to handle challenging CoSOD datasets, for the traditional method based on color histogram, *i.e.*, CBCD, we may also find that CBCD is much more robust to noise than exposure tuning, since it shows a lower performance for “w/o noise” than “w/o exposure”. In contrast to CBCD, the other three deep methods are more sensitive to noise.

4.3 Comparison with Existing Attacks

Baselines. We consider a series of additive-perturbation-noise attacks as baselines, *i.e.*, FGSM (Goodfellow, Shlens, and Szegedy 2014), I-FGSM (Kurakin, Goodfellow, and

	GICD				GCAGC				CBCD				PoolNet			
	S \uparrow	AP \downarrow	F_β \downarrow	MAE \uparrow	S \uparrow	AP \downarrow	F_β \downarrow	MAE \uparrow	S \uparrow	AP \downarrow	F_β \downarrow	MAE \uparrow	S \uparrow	AP \downarrow	F_β \downarrow	MAE \uparrow
Original	0.2352	0.8595	0.7800	0.0838	0.1881	0.8960	0.8275	0.0814	0.9504	0.6046	0.1530	0.2287	0.2625	0.8449	0.7626	0.1001
Noise ₈	0.2238	0.8602	0.7863	0.0841	0.2074	0.8893	0.8179	0.0868	0.9464	0.6057	0.1535	0.2283	0.2655	0.8432	0.7628	0.1011
Noise ₁₆	0.2367	0.8525	0.7734	0.0886	0.2323	0.8779	0.8009	0.0950	0.9504	0.6054	0.1476	0.2289	0.2844	0.8358	0.7521	0.1048
Noise ₃₂	0.3012	0.8216	0.7310	0.1048	0.2988	0.8395	0.7519	0.1200	0.9598	0.5953	0.1376	0.2313	0.3429	0.8144	0.7078	0.1145
FGSM _{BCE}	0.4422 *	0.7644 *	0.6366 *	0.1351 *	0.3355	0.8309	0.7315	0.1295	0.9543	0.5961	0.1503	0.2302	0.3454	0.8089	0.7043	0.1175
FGSM _{L₁}	0.4561 *	0.7655 *	0.6098 *	0.1410 *	0.3300	0.8342	0.7384	0.1294	0.9573	0.5982	0.1458	0.2302	0.3524	0.8077	0.6998	0.1168
I-FGSM _{BCE}	0.7285 *	0.6510 *	0.3970 *	0.3337 *	0.2769	0.8455	0.7644	0.1146	0.9533	0.6042	0.1491	0.2286	0.2754	0.8339	0.7503	0.1057
I-FGSM _{L₁}	0.6397 *	0.6561 *	0.5134 *	0.2700 *	0.2615	0.8643	0.7801	0.1063	0.9454	0.6059	0.1533	0.2280	0.2715	0.8364	0.7533	0.1052
MI-FGSM _{BCE}	0.6700 *	0.6697 *	0.4480 *	0.2868 *	0.3975	0.7909	0.6842	0.1532	0.9514	0.5995	0.1468	0.2293	0.3375	0.8009	0.6976	0.1215
MI-FGSM _{L₁}	0.5921 *	0.6541 *	0.5543 *	0.2331 *	0.3598	0.8193	0.7130	0.1355	0.9548	0.6024	0.1508	0.2294	0.3266	0.8113	0.7142	0.1180
TI-MI-FGSM _{BCE}	0.5380 *	0.7206 *	0.5371 *	0.2112 *	0.3146	0.8197	0.7322	0.1316	0.9623	0.5648	0.1504	0.2318	0.3628	0.7894	0.6784	0.1236
TI-MI-FGSM _{L₁}	0.4903 *	0.7247 *	0.6074 *	0.1789 *	0.3097	0.8378	0.7514	0.1234	0.9583	0.5677	0.1500	0.2315	0.3489	0.8050	0.6900	0.1190
Jadena _{single}	0.6864	0.7044	0.3831	0.1753	0.4868	0.7682	0.6162	0.1529	0.9663	0.5490	0.1199	0.2354	0.5538	0.6985	0.5152	0.1431
Jadena _{group}	0.6849	0.7069	0.3838	0.1777	0.5221	0.7453	0.5842	0.1619	0.9826	0.5212	0.0715	0.2392	0.6060	0.6671	0.4650	0.1545
Jadena _{augment}	0.6893	0.7016	0.3747	0.1749	0.5146	0.7432	0.5960	0.1592	0.9816	0.5137	0.0754	0.2394	0.6010	0.6648	0.4616	0.1513

Table 2: Comparison with existing attacks. Noise _{ϵ} s apply random additive noise sampled from uniform distribution $U(-\epsilon, \epsilon)$ on each channel of images. The attacks of FGSM and *FGSMs are performed against co-saliency labels and have full access to the network structure and parameters of the GICD model. *_{BCE, L₁} means that the adopted adversarial loss is binary cross-entropy (BCE) loss or the L_1 loss. We mark white-box attacks with star and highlight top 3 results with **red**, **green**, and **blue** respectively.

Bengio 2016), MI-FGSM (Dong et al. 2018), TI-MI-FGSM (Dong et al. 2019). For the hyperparameters of baselines, we set the max perturbation $\epsilon = 16$ with pixel values in $[0, 255]$ respectively, as well as iteration number $N = 20$, step size $\alpha_n = 1$ for iteration attacks, momentum decay $\mu = 1.0$ for momentum methods, and Gaussian kernel length to be 15 for TI-MI-FGSM. Since no specific attacks for CoSOD methods were proposed, we follow a general white-box attack manner and employ L_1 norm and binary cross-entropy (BCE) as adversarial losses.

Attack comparison. We launch baselines and our method on Cosal2015 dataset. The hyperparameters of our method follow Sec. 4.2. The comparison results are shown in Tab. 2.

Compared with existing additive-perturbation-based attacks, our proposed Jedena outperforms all of them except for white-box attacks, which suggests better transferability of our method than baselines. Since we only borrow several shallow layers from the deep classification model, our proposed method needs less computation cost than an iterative attack method with a result-based adversarial loss, which unavoidably back-propagates gradients through the whole deep model.

Image quality comparison. We also evaluate the image quality of generated adversarial examples and investigate how distortion degree affects the attack performance. For each attack method, we plot a line to describe the Success Rate vs. BRISQUE in Fig. 3 by changing the maximum noise perturbation ϵ_n and λ_b for our method as well. We also show some cases to visualize how attack method perturb an image in Fig. 4. For baselines attacks, we follow the default settings of the above section, but only use the BCE loss since it usually has a better performance than L_1 loss. For our method, we adopt the variant of “augment”, i.e., Jadena_{augment}, which is practical and convenient to perform in a real-world scenery.

We have three findings: ❶ compared with white-box attacks for GICD, our method has a competitive performance

with MI-FGSM, and outperforms FGSM. ❷ when transferred to GCAGC and PoolNet, our method outperforms most additive-perturbation-based methods except for TI-MI-FGSM. Especially for PoolNet a single saliency detector, our method shows significant advantages beyond FGSM, I-FGSM and MI-FGSM, which is reasonable for them being adversarial against a CoSOD method and showing lower transferability for a SOD method than our proposed black-box attack. ❸ we also notice that TI-MI-FGSM applies coarse-graining and local smoothing noises on images unlike ordinary noises as shown in the last row of Fig. 4, which looks unnatural for human, but fools BRISQUE measure.

5 Conclusions

In this work, we have investigated a novel problem: how to effectively protect personal-sensitive image contents from being extracted or discovered by the state-of-the-art co-saliency object detection methods. We have addressed this problem from the perspective of adversarial attack and identified a novel task, i.e., adversarial co-saliency attack that aims at tackling the following scenarios: given an image selected from an image group containing some common and salient objects, how to generate an adversarial version of the image that can mislead CoSOD methods to predict incorrect co-salient regions, thus evading the co-saliency detection and making the images undiscoverable by the co-saliency detection algorithms. We have proposed the very first blackbox *joint adversarial exposure & noise attack* (Jadena) where we jointly and locally tune the exposure and additive perturbations of the image according to a newly designed *high-feature-level contrast-sensitive loss* function. Our method, without needing any information of the state-of-the-art CoSOD methods, leads to significant performance degradation on various co-saliency detection datasets and makes the co-salient objects undetectable. The effectiveness of the proposed method is thoroughly validated and showcased through various quantitative and qualitative experiments. We believe that the proposed method can greatly

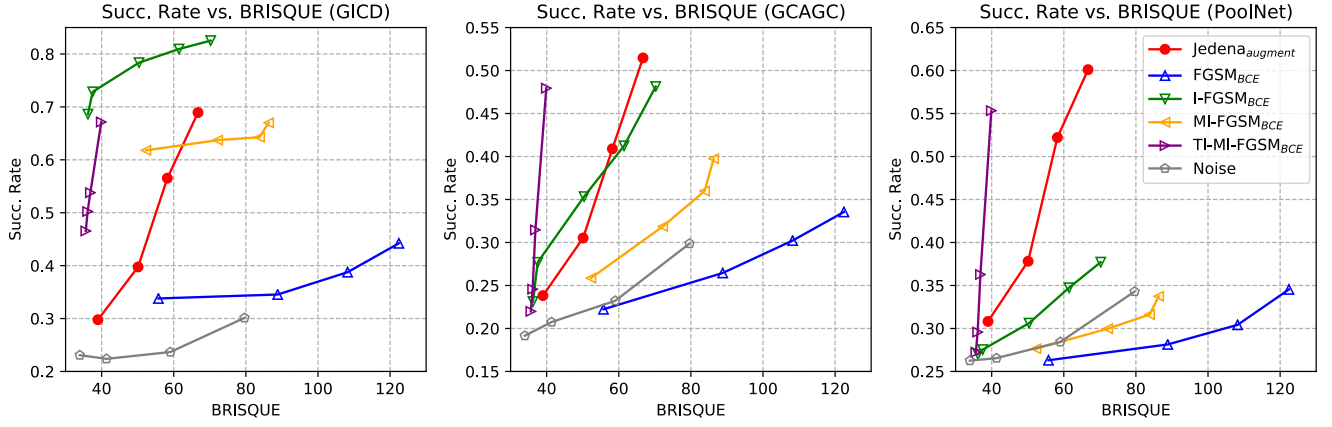


Figure 3: Success Rate vs. BRISQUE. This figure shows the change in success rate of attacks with the distortion degree. A larger BRISQUE suggests a worse quality of images, *i.e.*, more distortion. The performance of our method is plotted in red.

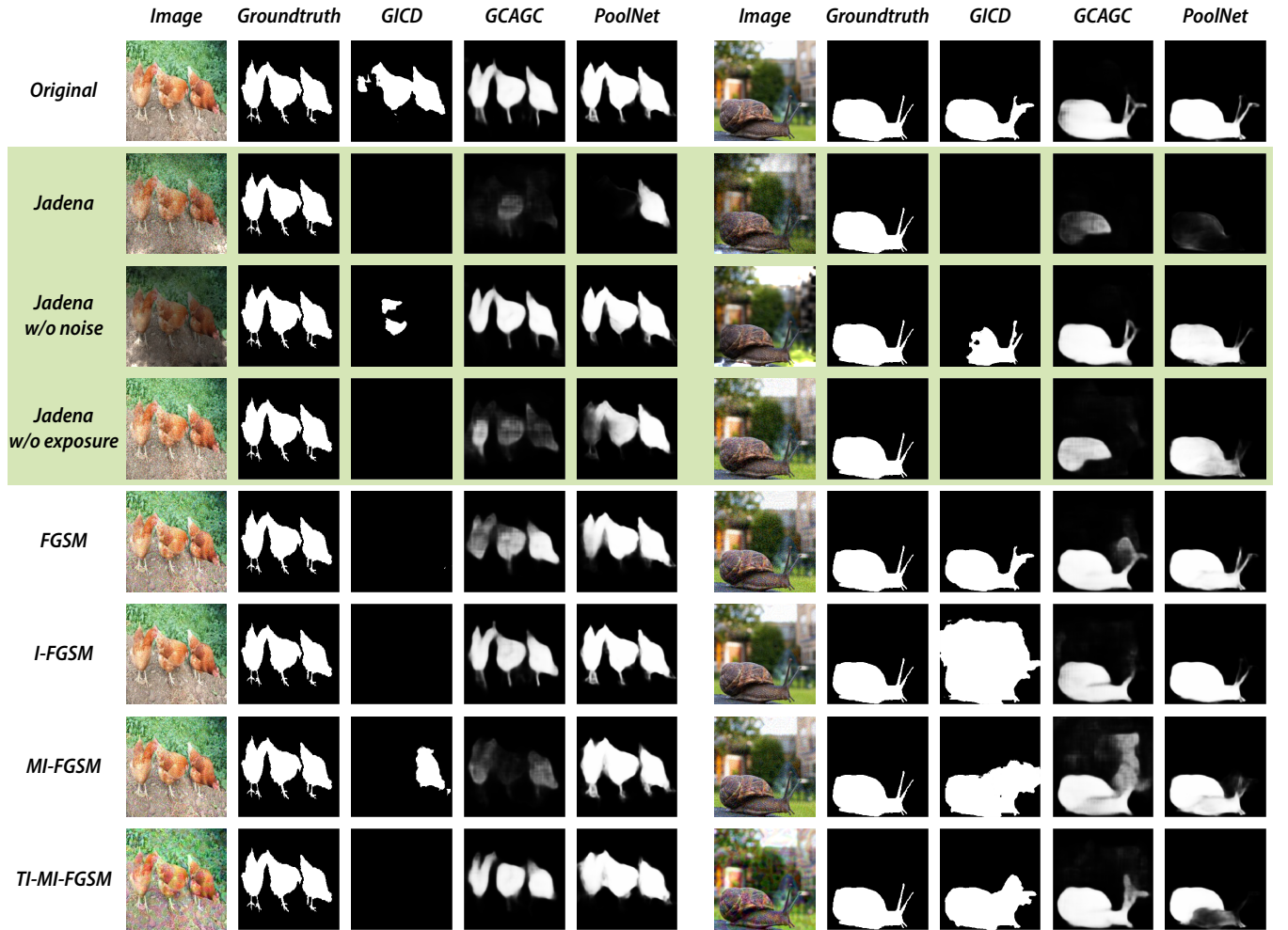


Figure 4: Visualization of attack results. We show two cases from Cosal2015 dataset in this figure. We visualize the image, the ground-truth of co-saliency map and results of GICD, GCAGC and PoolNet along columns, and show the images perturbed by Jadana, FGSM, I-FGSM, MI-FGSM, TI-MI-FGSM and corresponding results, besides the original ones, for each row. We highlight our method in green.

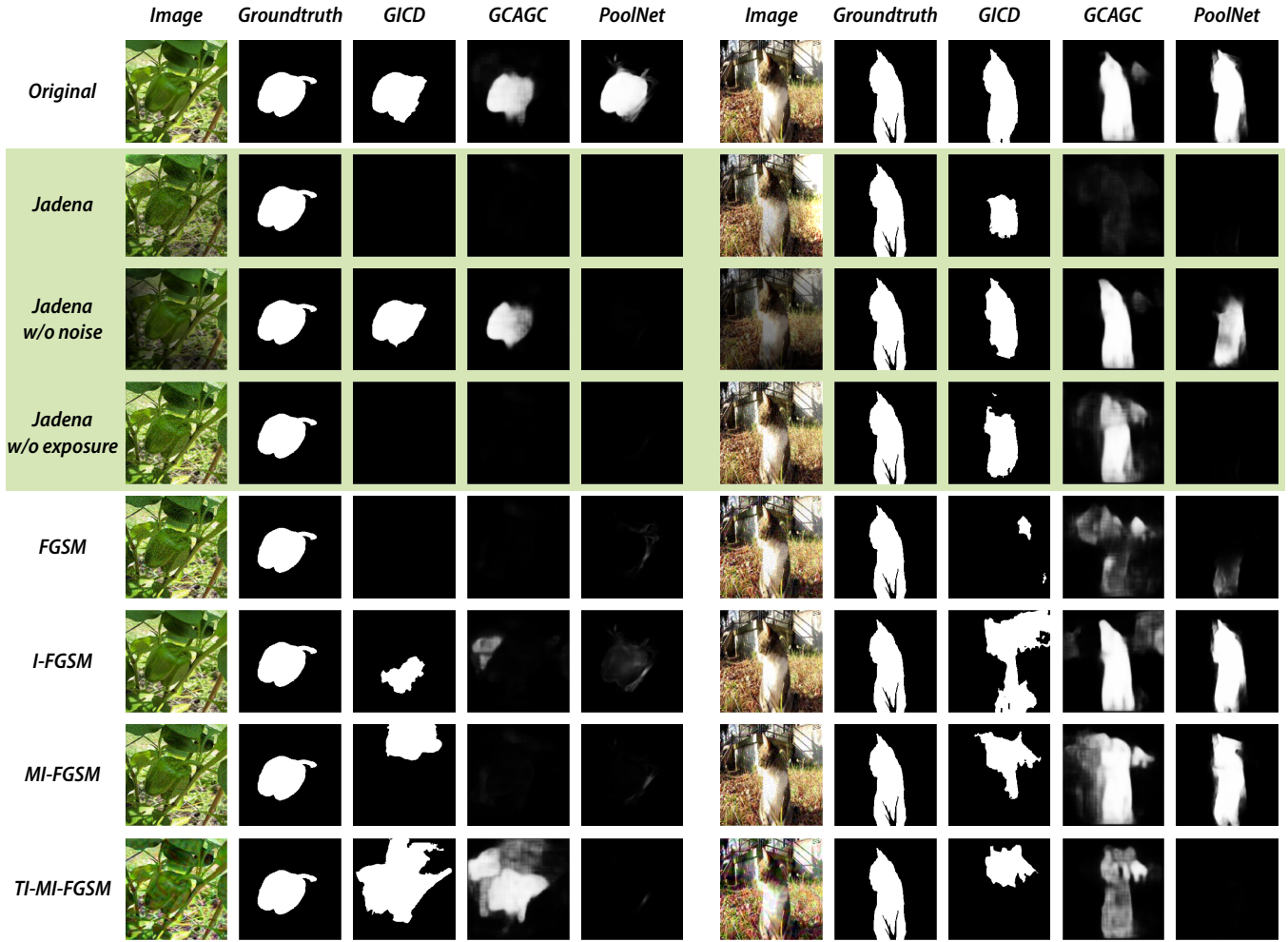


Figure I: More visualization results from Cosal2015. We visualize the image, the ground-truth of co-saliency map and results of GICD, GCAGC and PoolNet along columns, and show the original images and images perturbed by Jadena, baselines followed by corresponding results for each row. We highlight our method in green.

benefit the design and execution of privacy-oriented content sharing on the public domain where malicious extractions can be effectively inhibited.

In future work, we would like to further extend the proposed Jadena to a more broad range of applications, such as object segmentation (Guo et al. 2018, 2017c) and visual object tracking (Guo et al. 2020a,c, 2017a; Chen et al. 2018; Guo et al. 2017b). Moreover, we will use our adversarial exposure attack as a new kind of mutation for DNN testing (Xie et al. 2019a; Du et al. 2019; Xie et al. 2019b; Ma et al. 2018). Not being a traditional noise-based adversarial attack, it is quite worthwhile to investigate the interplay between the proposed Jadena and other non-additive-noise based attack modes such as (Zhai et al. 2020; Guo et al. 2020c; Wang et al. 2020; Guo et al. 2020b; Cheng et al. 2020).

Appendix

In this appendix, we present more visualization results of baselines and our attack method across CoSOD methods, to demonstrate the advantages of ours over baselines.

We show more visualization results of cases from Cosal2015 (Zhang et al. 2016) in Figs. I and II, and ones from CoSOD3k (Fan et al. 2020) in Figs. III and IV. All hyperparameter settings and the layout keep the same with Fig. 4 of the main paper.

We may observe adversarial examples generated by our proposed method hold more transferability across CoSOD methods, without perceptible perturbation. Moreover, visualization results validate the joint perturbations play an important role in fooling CoSOD methods, since our method with joint perturbations outperforms “w/o noise” and “w/o exposure” versions. We can also notice that TI-MI-FGSM applies unnatural noise, which is more perceptible than any other noise-based attacks.

References

Achanta, R.; Hemami, S.; Estrada, F.; and Susstrunk, S. 2009. Frequency-Tuned Salient Region Detection. In *Proceedings of the IEEE Conference on Computer Vision and Pattern Recognition*, 1597–1604.

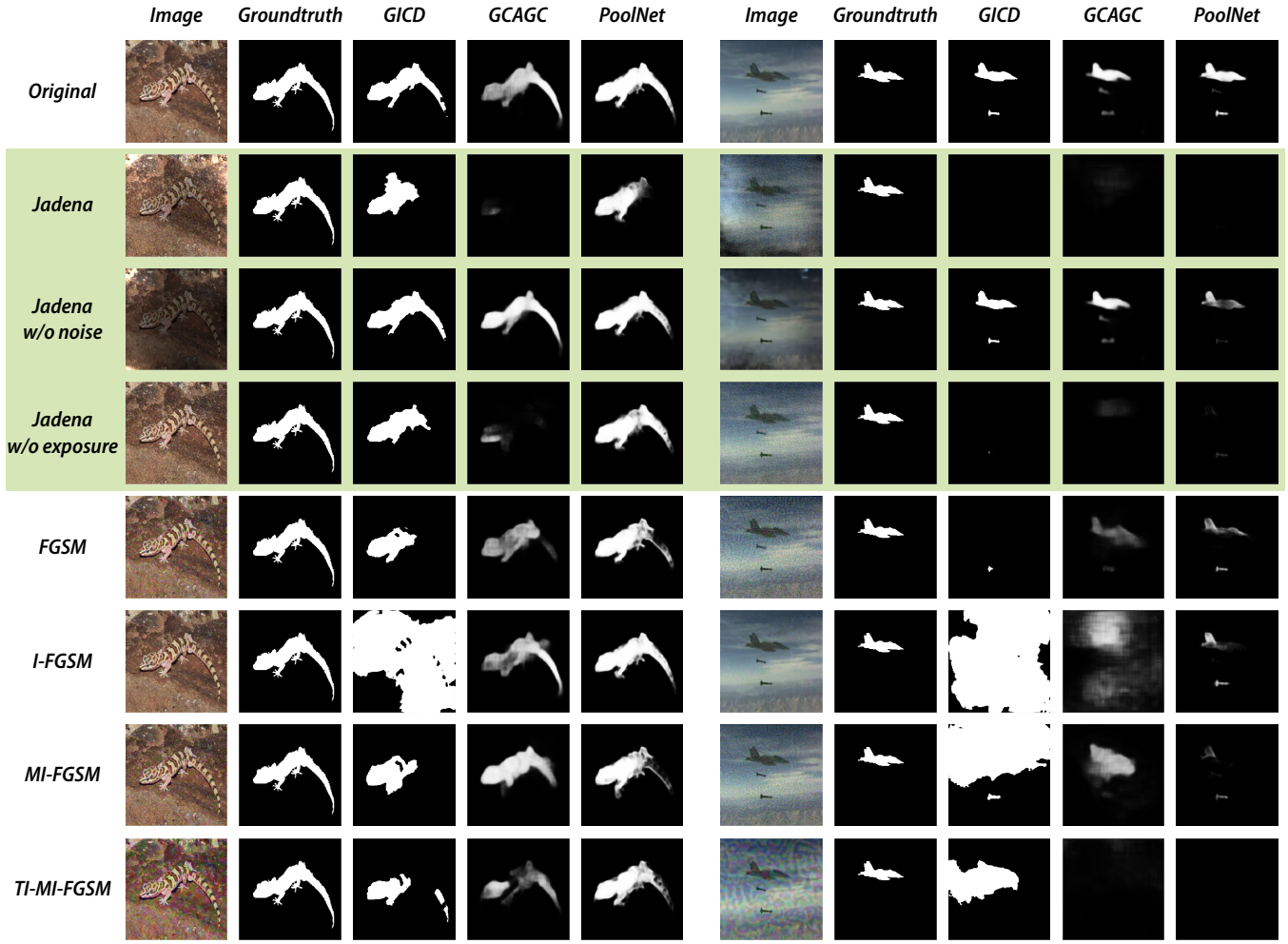


Figure II: More visualization results from Cosal2015. We visualize the image, the ground-truth of co-saliency map and results of GICD, GCAGC and PoolNet along columns, and show the original images and images perturbed by Jadena, baselines followed by corresponding results for each row. We highlight our method in green.

Batra, D.; Kowdle, A.; Parikh, D.; Luo, J.; and Chen, T. 2010. iCoseg: Interactive Co-Segmentation with Intelligent Scribble Guidance. In *Proceedings of the IEEE Conference on Computer Vision and Pattern Recognition*, 3169–3176.

Cao, X.; Tao, Z.; Zhang, B.; Fu, H.; and Feng, W. 2014. Self-Adaptively Weighted Co-Saliency Detection via Rank Constraint. *IEEE Transactions on Image Processing* 23(9): 4175–4186.

Carlini, N.; and Wagner, D. 2017. Towards Evaluating the Robustness of Neural Networks. In *IEEE Symposium on Security and Privacy*, 39–57. IEEE.

Chang, X.; Yang, Y.; Xing, E.; and Yu, Y. 2015. Complex Event Detection Using Semantic Saliency and Nearly-Isotonic SVM. In *International Conference on Machine Learning*, 1348–1357.

Che, Z.; Borji, A.; Zhai, G.; Ling, S.; Guo, G.; and Callet, P. L. 2019. Adversarial Attacks against Deep Saliency Models. *arXiv preprint arXiv:1904.01231*.

Chen, Z.; Guo, Q.; Wan, L.; and Feng, W. 2018. Background-suppressed correlation filters for visual tracking. In *Proceedings of the IEEE International Conference on Multimedia and Expo*, 1–6. IEEE.

Cheng, M.-M.; Mitra, N.; Huang, X.; Torr, P.; and Hu, S.-M. 2015. Global Contrast Based Salient Region Detection. *IEEE Transactions on Pattern Analysis and Machine Intelligence* 37(3): 569–582.

Cheng, M.-M.; Mitra, N. J.; Huang, X.; and Hu, S.-M. 2014. Salienshape: Group Saliency in Image Collections. *The Visual Computer* 30(4): 443–453.

Cheng, Y.; Guo, Q.; Juefei-Xu, F.; Xie, X.; Lin, S.-W.; Lin, W.; Feng, W.; and Liu, Y. 2020. Pasadena: Perceptually Aware and Stealthy Adversarial Denoise Attack. *arXiv preprint arXiv:2007.07097*.

Cong, R.; Lei, J.; Fu, H.; Cheng, M.-M.; Lin, W.; and Huang, Q. 2018. Review of Visual Saliency Detection with Comprehensive Information. *IEEE Transactions on Circuits and Systems for Video Technology*.

Dong, Y.; Liao, F.; Pang, T.; Su, H.; Zhu, J.; Hu, X.; and Li, J. 2018. Boosting Adversarial Attacks with Momentum. In *Proceedings of the IEEE Conference on Computer Vision and Pattern Recognition*, 9185–9193.

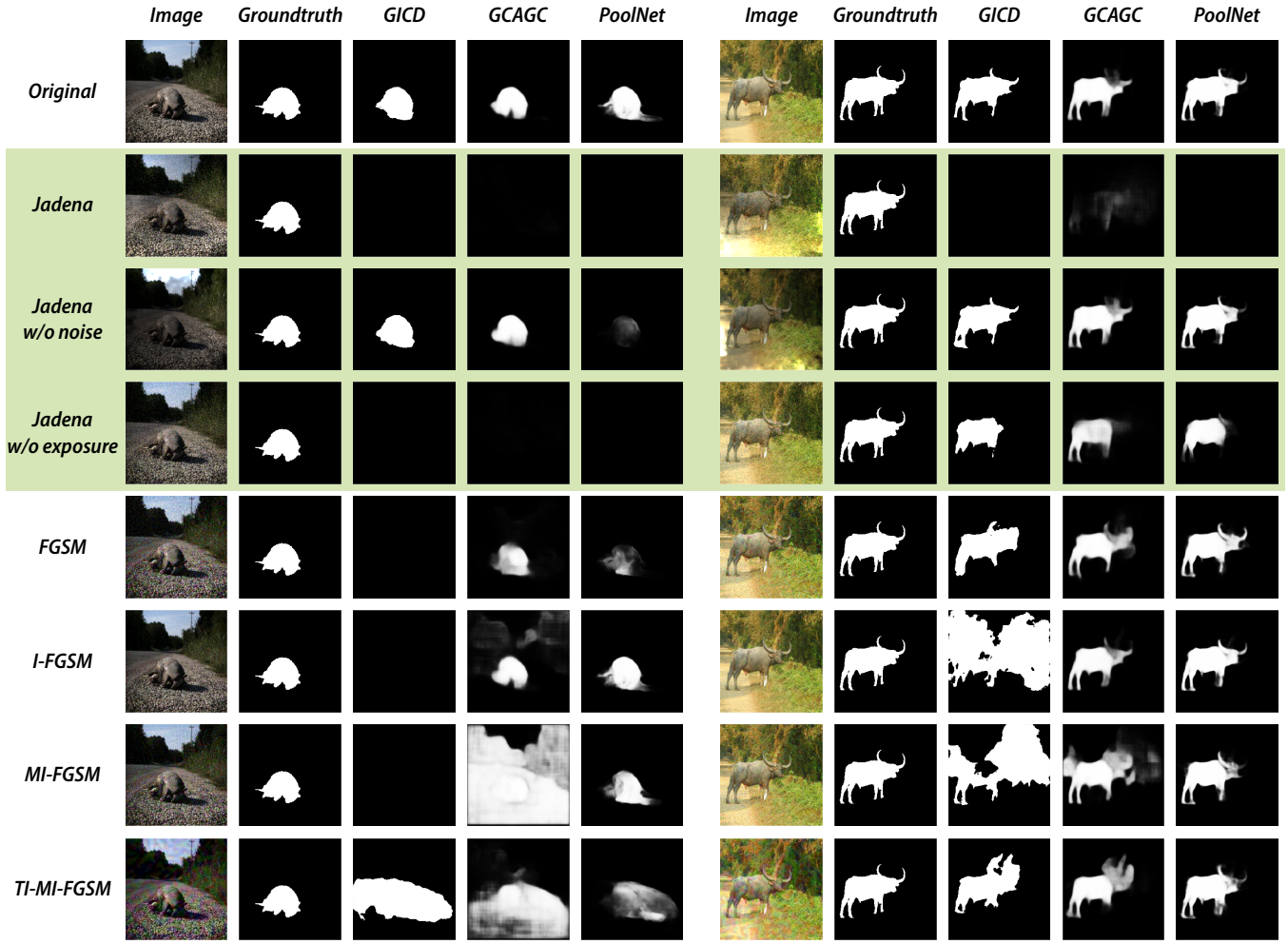


Figure III: More visualization results from CoSOD3k. We visualize the image, the ground-truth of co-saliency map and results of GICD, GCAGC and PoolNet along columns, and show the original images and images perturbed by Jadena, baselines followed by corresponding results for each row. We highlight our method in green.

Dong, Y.; Pang, T.; Su, H.; and Zhu, J. 2019. Evading Defenses to Transferable Adversarial Examples by Translation-Invariant Attacks. In *Proceedings of the IEEE Conference on Computer Vision and Pattern Recognition*.

Du, X.; Xie, X.; Li, Y.; Ma, L.; Liu, Y.; and Zhao, J. 2019. Deepstellar: Model-based quantitative analysis of stateful deep learning systems. In *Proceedings of the ACM Joint Meeting on European Software Engineering Conference and Symposium on the Foundations of Software Engineering*, 477–487.

Fan, D.-P.; Lin, Z.; Ji, G.-P.; Zhang, D.; Fu, H.; and Cheng, M.-M. 2020. Taking a Deeper Look at the Co-Salient Object Detection. In *Proceedings of the IEEE Conference on Computer Vision and Pattern Recognition*.

Fu, H.; Cao, X.; and Tu, Z. 2013. Cluster-Based Co-Saliency Detection. *IEEE Transactions on Image Processing* 22(10): 3766–3778.

Fu, X.; Zeng, D.; Huang, Y.; Zhang, X.-P.; and Ding, X. 2016. A Weighted Variational Model for Simultaneous Reflectance and Illumination Estimation. In *Proceedings of the IEEE Conference on Computer Vision and Pattern Recognition*, 2782–2790.

Ge, C.; Fu, K.; Liu, F.; Bai, L.; and Yang, J. 2016. Co-Saliency Detection via Inter and Intra Saliency Propagation. *Signal Processing: Image Communication* 44: 69–83.

Goodfellow, I. J.; Shlens, J.; and Szegedy, C. 2014. Explaining and Harnessing Adversarial Examples. *arXiv preprint arXiv:1412.6572*.

Guo, Q.; Feng, W.; Zhou, C.; Huang, R.; Wan, L.; and Wang, S. 2017a. Learning dynamic siamese network for visual object tracking. In *Proceedings of the IEEE International Conference on Computer Vision*, 1763–1771.

Guo, Q.; Feng, W.; Zhou, C.; Pun, C.-M.; and Wu, B. 2017b. Structure-regularized compressive tracking with online data-driven sampling. *IEEE Transactions on Image Processing* 26(12): 5692–5705.

Guo, Q.; Han, R.; Feng, W.; Chen, Z.; and Wan, L. 2020a. Selective spatial regularization by reinforcement learned decision making for object tracking. *IEEE Transactions on Image Processing* 29: 2999–3013.



Figure IV: More visualization results from CoSOD3k. We visualize the image, the ground-truth of co-saliency map and results of GICD, GCAGC and PoolNet along columns, and show the original images and images perturbed by Jadena, baselines followed by corresponding results for each row. We highlight our method in green.

Guo, Q.; Juefei-Xu, F.; Xie, X.; Ma, L.; Wang, J.; Feng, W.; and Liu, Y. 2020b. ABBA: Saliency-Regularized Motion-Based Adversarial Blur Attack. *arXiv preprint arXiv:2002.03500*.

Guo, Q.; Sun, S.; Dong, F.; Feng, W.; Gao, B. Z.; and Ma, S. 2017c. Frequency-tuned ACM for biomedical image segmentation. In *Proceedings of the IEEE International Conference on Acoustics, Speech and Signal Processing*, 821–825. IEEE.

Guo, Q.; Sun, S.; Ren, X.; Dong, F.; Gao, B. Z.; and Feng, W. 2018. Frequency-tuned active contour model. *Neurocomputing* 275: 2307–2316.

Guo, Q.; Xie, X.; Juefei-Xu, F.; Ma, L.; Li, Z.; Xue, W.; Feng, W.; and Liu, Y. 2020c. SPARK: Spatial-aware online incremental attack against visual tracking. In *Proceedings of the European Conference on Computer Vision*.

He, K.; Zhang, X.; Ren, S.; and Sun, J. 2016. Deep Residual Learning for Image Recognition. In *Proceedings of the IEEE Conference on Computer Vision and Pattern Recognition*, 770–778.

Jerriophthula, K. R.; Cai, J.; and Yuan, J. 2018. Quality-Guided Fusion-Based Co-Saliency Estimation for Image Co-Segmentation

and Colocalization. *IEEE Transactions on Multimedia* 20(9): 2466–2477.

Jia, X.; Wei, X.; Cao, X.; and Han, X. 2020. Adv-Watermark: A Novel Watermark Perturbation for Adversarial Examples. *arXiv preprint arXiv:2008.01919*.

Jiang, B.; Jiang, X.; Zhou, A.; Tang, J.; and Luo, B. 2019. A Unified Multiple Graph Learning and Convolutional Network Model for Co-Saliency Estimation. In *Proceedings of the ACM International Conference on Multimedia*, 1375–1382.

Kar, A.; Tulsiani, S.; Carreira, J.; and Malik, J. 2015. Category-Specific Object Reconstruction from a Single Image. In *Proceedings of the IEEE Conference on Computer Vision and Pattern Recognition*, 1966–1974.

Kurakin, A.; Goodfellow, I.; and Bengio, S. 2016. Adversarial Examples in the Physical World. *arXiv preprint arXiv:1607.02533*.

Li, B.; Sun, Z.; Tang, L.; Sun, Y.; and Shi, J. 2019. Detecting Robust Co-Saliency with Recurrent Co-Attention Neural Network. In *Proceedings of the IEEE Conference on International Joint Conferences on Artificial Intelligence*, 818–825.

- Li, G.; and Yu, Y. 2015. Visual Saliency Based on Multiscale Deep Features. In *Proceedings of the IEEE Conference on Computer Vision and Pattern Recognition*, 5455–5463.
- Li, G.; and Yu, Y. 2016. Deep Contrast Learning for Salient Object Detection. In *Proceedings of the IEEE Conference on Computer Vision and Pattern Recognition*.
- Li, H.; Meng, F.; Luo, B.; and Zhu, S. 2014. Repairing Bad Co-Segmentation Using Its Quality Evaluation and Segment Propagation. *IEEE Transactions on Image Processing* 23(8): 3545–3559.
- Liu, J.-J.; Hou, Q.; Cheng, M.-M.; Feng, J.; and Jiang, J. 2019. A Simple Pooling-Based Design for Real-Time Salient Object Detection. In *Proceedings of the IEEE Conference on Computer Vision and Pattern Recognition*.
- Luo, Y.; Jiang, M.; Wong, Y.; and Zhao, Q. 2015. Multi-Camera Saliency. *IEEE Transactions on Pattern Analysis and Machine Intelligence* 37(10): 2057–2070.
- Ma, L.; Juefei-Xu, F.; Sun, J.; Chen, C.; Su, T.; Zhang, F.; Xue, M.; Li, B.; Li, L.; Liu, Y.; Zhao, J.; and Wang, Y. 2018. DeepGauge: Multi-Granularity Testing Criteria for Deep Learning Systems. In *Proceedings of the IEEE/ACM International Conference on Automated Software Engineering*.
- Mittal, A.; Moorthy, A. K.; and Bovik, A. C. 2011. Blind/Referenceless Image Spatial Quality Evaluator. In *Asilomar Conference on Signals, Systems and Computers*, 723–727.
- Qin, X.; Zhang, Z.; Huang, C.; Gao, C.; Dehghan, M.; and Jagersand, M. 2019. BASNet: Boundary-Aware Salient Object Detection. In *Proceedings of the IEEE conference on computer vision and pattern recognition*.
- Song, S.; Yu, H.; Miao, Z.; Fang, J.; Zheng, K.; Ma, C.; and Wang, S. 2020. Multi-Spectral Salient Object Detection by Adversarial Domain Adaptation. In *Proceedings of the AAAI Conference on Artificial Intelligence*.
- Tang, K.; Joulain, A.; Li, L.-J.; and Fei-Fei, L. 2014. Co-Localization in Real-World Images. In *Proceedings of the IEEE Conference on Computer Vision and Pattern Recognition*, 1464–1471.
- Tran, R.; Patrick, D.; Geyer, M.; and Fernandez, A. 2020. SAD: Saliency-Based Defenses against Adversarial Examples. *arXiv preprint arXiv:2003.04820*.
- Wang, J.; Sun, K.; Cheng, T.; Jiang, B.; Deng, C.; Zhao, Y.; Liu, D.; Mu, Y.; Tan, M.; Wang, X.; Liu, W.; and Xiao, B. 2019. Deep High-Resolution Representation Learning for Visual Recognition. *IEEE Transactions on Pattern Analysis and Machine Intelligence*.
- Wang, L.; Wang, L.; Lu, H.; Zhang, P.; and Ruan, X. 2016. Saliency Detection with Recurrent Fully Convolutional Networks. In *European Conference on Computer Vision*, 825–841.
- Wang, R.; Juefei-Xu, F.; Guo, Q.; Huang, Y.; Xie, X.; Ma, L.; and Liu, Y. 2020. Amora: Black-box Adversarial Morphing Attack. In *Proceedings of the ACM International Conference on Multimedia*.
- Xie, X.; Ma, L.; Juefei-Xu, F.; Xue, M.; Chen, H.; Liu, Y.; Zhao, J.; Li, B.; Yin, J.; and See, S. 2019a. DeepHunter: A Coverage-Guided Fuzz Testing Framework for Deep Neural Networks. In *Proceedings of the ACM SIGSOFT International Symposium on Software Testing and Analysis*.
- Xie, X.; Ma, L.; Wang, H.; Li, Y.; Liu, Y.; and Li, X. 2019b. DiffChaser: Detecting Disagreements for Deep Neural Networks. In *Proceedings of the International Joint Conference on Artificial Intelligence*, 5772–5778.
- Yu, H.; Zheng, K.; Fang, J.; Guo, H.; Feng, W.; and Wang, S. 2018. Co-Saliency Detection Within a Single Image. In *Proceedings of the AAAI Conference on Artificial Intelligence*.
- Zha, Z.-J.; Wang, C.; Liu, D.; Xie, H.; and Zhang, Y. 2020. Robust Deep Co-Saliency Detection with Group Semantic and Pyramid Attention. *IEEE Transactions on Neural Networks and Learning Systems*.
- Zhai, L.; Juefei-Xu, F.; Guo, Q.; Xie, X.; Ma, L.; Feng, W.; Qin, S.; and Liu, Y. 2020. It’s Raining Cats or Dogs? Adversarial Rain Attack on DNN Perception. *arXiv preprint arXiv*.
- Zhang, D.; Fu, H.; Han, J.; Borji, A.; and Li, X. 2018. A Review of Co-Saliency Detection Algorithms: Fundamentals, applications, and challenges. *ACM Transactions on Intelligent Systems and Technology* 9(4): 1–31.
- Zhang, D.; Han, J.; Li, C.; Wang, J.; and Li, X. 2016. Detection of Co-Salient Objects by Looking Deep and Wide. *International Journal of Computer Vision* 120(2): 215–232.
- Zhang, D.; Meng, D.; Li, C.; Jiang, L.; Zhao, Q.; and Han, J. 2015. A Self-Paced Multiple-Instance Learning Framework for Co-Saliency Detection. In *Proceedings of the IEEE International Conference on Computer Vision*, 594–602.
- Zhang, K.; Li, T.; Shen, S.; Liu, B.; Chen, J.; and Liu, Q. 2020a. Adaptive Graph Convolutional Network with Attention Graph Clustering for Co-Saliency Detection. In *Proceedings of the IEEE Conference on Computer Vision and Pattern Recognition*, 9050–9059.
- Zhang, Q.; Nie, Y.; Zhu, L.; Xiao, C.; and Zheng, W.-S. 2020b. Enhancing Underexposed Photos using Perceptually Bidirectional Similarity. *IEEE Transactions on Multimedia* 1–1.
- Zhang, Z.; Jin, W.; Xu, J.; and Cheng, M.-M. 2020c. Gradient-Induced Co-Saliency Detection. In *European Conference on Computer Vision*.
- Zhu, H.; Meng, F.; Cai, J.; and Lu, S. 2016. Beyond Pixels: A Comprehensive Survey from Bottom-Up to Semantic Image Segmentation and Cosegmentation. *Journal of Visual Communication and Image Representation* 34: 12–27.